COVER SHEET

ION GPS-95 Meeting
September 12-15,1995

SESSION:

B4: Earth Observation and Timing

SESSION DATE:

Sep. 14, 1995

AUTHOR NAME(S) & AFFILIATION:

George A. Hajj
E. Rob Kursinski
Willy I. Bertiger
Stephen S. Leroy
Larry J. Remans
J. Tim Schofield

all at : Jet Propulsion Lab
4800 Oak Grove Dr.
Pasadena, CA 91109

TITLE OF PAPER:

Initial Verification of the GPS-LEO Occultation Technique of Mapping the Atmosphere with the GPS-MET Experiment

BIOGRAPHIES

Dr. George Hajj is a Member of the Technical Staff at the Jet Propulsion Laboratory in the Tracking Systems and Applications Section. He received his Ph.D. in physics from Rice University in 1988. His research experience. and interests are in the areas of radio propagation and scattering, tomographic imaging, and GPS radio occultation techniques and applications.

E. Rob Kursinski is a member of the Technical Staff in the Earth and Space Sciences Division. He is pursuing a Ph.D. in Planetary Science at the California Institute of Technology and has an extensive background in the application of radio occultation instrumentation and techniques to the remote sounding of planetary atmospheres. His current interests are in applying the GPS radio occultation techniques to study the Earth's atmosphere.

Dr. Winy Bertiger received his Ph.D. in Mathematics from the University of California, Berkeley, in 1976 specializing in Partial Differential Equations. Hc is currently a Member of the Technical Staff at the Jet Propulsion Laboratory in the Tracking Systems and Applications Section. 11 is work at JPL has been focused on the use of GPS for high precision orbit determination.

Dr. Stephen Leroy is a postdoctoral associate in the Earth and Space Sciences Division at the Jet Propulsion Laboratory. He received his Ph.D. in planetary science from the California Institute of Technology and his primary interests arc in atmospheric waves and the climatology of the middle and lower atmosphere.

Dr. Larry Romans received his Ph.D. in theoretical physics from Caltech in 1985. Hc is currently a Member of the Technical Staff in the Space Geodesy and Geodynamics Group at JPL, where his work has focused on geodetic applications of G] 'S.

Dr. Tim Schofield is a Member of Technical Staff in the Earth and Space Sciences Division. He received his D. Phil. in atmospheric physics at the University of Oxford and his primary interest is the remote sounding of atmospheres.

ABSTRACT

The radio occultation technique, which has been repeatedly proven for planetary atmospheres, was first utilized to observe Earth's atmosphere by the GPS-MET experiment (launched in April 1995), in which a high performance GPS receiver was placed into a low-Earth orbit. During certain phases of the mission, more than 100 occultations per day are acquired. A subset of this occultation data is analyzed and temperature in the neutral atmosphere and electron profiles in the ionosphere are obtained. Comparing about 100 (31' S-M ET retrievals to accurate meteorological analyses obtained from the European Center for Medium-range Weather Forecasting at heights between 5-30 km, temperature differences display biases of less than 0.5K and standard deviations of 1 -2K in the northern hemisphere, where the model is expected to be most accurate. Furthermore, electron density profiles obtained for different geodetic locations and times show the main features that arc expected in the ionosphere.

1-INTRODUCTION

When a signal transmitted by the global positioning system (GPS) and received by a low-Earth orbiter (LEO) passes through the Earth's atmosphere [Fig. 1] its phase and amplitude arc affected in ways that arc characteristic of the index of refraction of the propagating medium. By applying certain assumptions on the variability of the index of refraction of the propagating media (e.g. spherical symmetry in the locality of the occultat ion), phase change measurements between the transmitter and the receiver yield refractivity profiles in the ionosphere (-60- 1000 km) and neutral atmosphere (0-50 km). The refractivity, in turn, yields electron density in the ionosphere, and temperature and pressure in the neutral atmosphere. In the

lower troposphere, where water vapor contribution to refractivity is appreciable, independent knowledge of the temperature can be used to solve for water vapor abundance.

The radio occultation technique has a 30 year tradition in NASA's planetary program and has been a part of the planetary exploration programs to Venus, Mars and the outer planets [see, for example, Tyler, 1987]. However, the application of the technique to sense the Earth's atmosphere using G] 'S, first suggested by Melbourne et al. [1988] and Yunck et al. [1988], was tested for the first time with the launch of the GPS-MET mission on April 3, 1995. GPS-MET is an experiment managed by the University Corporation of Atmospheric Research (UCAR) [Ware et al., 1995] and it consists of a 2. kg GPS receiver piggybacked on the Microl ab 1 satellite which has a circular orbit of 730 km altitude and 60° inclination. The GPS receiver is a space qualified TurboRogue [Meehan et al., 1992] capable of tracking up to 8 GPS satellites simultaneously at both frequencies transmitted by GPS. Under an optimal mode of operation, the GPS receiving antenna boresight is pointed in the negative velocity direct ion of the I .EO and provides 100-120 globally distributed setting occultations per day. By the end of the mission (nominal life time of 6 months), thousands of occultations will have been collected and can be used to assess the accuracy and potential benefit of the GPS radio occultations.

To date, a relatively small fraction of all recorded occultations have been analyzed using the Abel transform approach (presented below). This paper discusses how the GPS-MET data are analyzed and presents some results of temperat ore ret rievals compared to radiosonde measurements and atmospheric analyses obtained from the 1 European Center for Medium-range Weather Forecast (ECMWF). It also presents some preliminary results of electron density profiles obtained in the ionosphere. The paper is structured as follows: Section 2 gives a brief background on the radio occultation technique. The basic features of the technique are presented in section 3. The manner in which the GPS-MET phase data arc calibrated to isolate the atmospheric excess phase is described in section 4. Section 5 presents an individual temperature profile and statistics obtained for all occultations available from 2 days during the experiment. These retrievals are compared to atmospheric analysis from ECMWF. In section 6, wc show retrievals of ionospheric profiles obtained at different times of day and geographical locations. A conclusion is given in section '7.

2-'11111 RADIO OCCUI.TATION TECHNIQUE

The basic observable for each occultation is the phase change between the transmitter and the receiver as the signal descends through the ionosphere and the neutral atmosphere. After removal of geometrical effects due to the motion of the satellites and proper calibration of the transmitter and receiver clocks, the extra phase change induced by the atmosphere can be isolated. Excess atmospheric Doppler shift is then derived. This extra Doppler shift can be used to derive the atmospheric induced bending, α, as a function of the asymptote miss distance, a, [Fig. 1], Assuming a spherically symmetric atmosphere, the relation between the bending and excess Doppler shift, Δf, is given by

$$\Delta f = \frac{f}{c}\left[\vec{v}_t \cdot \hat{k}_t - \vec{v}_r \cdot \hat{k}_r + \left(\vec{v}_t - \vec{v}_r\right) \cdot \hat{k}\right], \quad (1)$$

where f is the operating frequency, c is the speed of light, $\vec{v}_t$ and $\vec{v}_r$ are the transmitter and receiver's velocity respect ively, $\hat{k}_t$ and $\hat{k}_r$ are the unit vectors in the direction of the transmitted and received signal respectively, $\hat{k}$ is the onit vector in the direction of the. straight line connecting the transmitter to the receiver.

The spherical symmetry assumption can also be used to relate the signal's bending to the medium's index of refract ion, n, via the relation

$$\alpha(a) = 2a\int_a^\infty \frac{1}{\sqrt{a'^2 - a^2}} \frac{d\ln(n)}{da'} da', \quad (2)$$

where $a = nr$ and t is the radius at the tangent point [Fig. 1], This integral equation can then be inverted by using an Abel integral transform given by

$$\ln(n(a)) = \frac{1}{\pi}\int_a^\infty \frac{\alpha(a')}{\sqrt{a'^2 - a^2}} da'. \quad (3)$$

The refractivity, N, is related to atmospheric quantities via

$$N = (n-1)\times 10^6 = 77.6\frac{P}{T} + 3.73\times 10^5 \frac{P_W}{T^2} - 40.3\times 10^6 \frac{n_e}{f^2}, \quad (4)$$

$$P = \frac{\rho R T}{m}, \quad (5)$$

$$\frac{\partial P}{\partial h} = -g\rho, \quad (6)$$

where P is total pressure (mbar), 7' is temperature (K), I'$_w$ is water vapor partial pressure (mbar), n_e is electron density (m^{-3}), f is operating frequency (Hz), ρ is density, R is the gas constant, m is the gas effective molecular weight, h is height, g is gravitational acceleration.

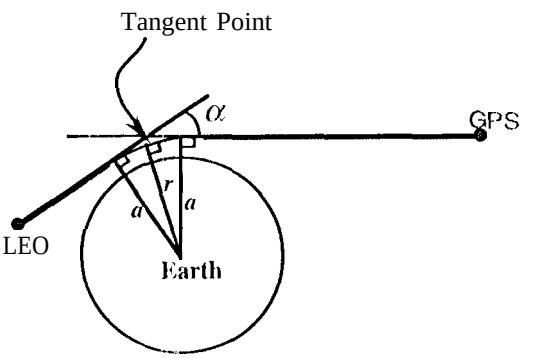

Fig. 1: Occultation geometry defining a, r, α and the tangent point.

When the signal is passing through the ionosphere (tangent point height > 60 km), use of a single GPS frequency is sufficient to estimate α to be used in Eq. (3). Moreover, the first two terms on the right hand side of Eq. (3) are negligible, therefore, knowledge of the index of refraction leads directly to electron density.

When the signal is going through both the neutral atmosphere and tbc ionosphere (tangent point height < 60 km), a linear combination of the two bending angles, associated with the two GPS frequencies, is used to isolate the *neutral* atmospheric bending and its refractivity profile is derived by usc of Eq. (3) [Vorob'ev and Krasil'nikova, 1993]. In the stratosphere and tbc region of the troposphere where temperature is colder than -250K, the water vapor term in Eq. (4) is negligible. Therefore, knowledge of refractivity yields the density of the medium by usc of the ideal gas law (Eq. 5). The density in turn yields the pressure by assuming hydrostatic equilibrium (Eq. 6) and a boundary condition at some height. Applying the gas law once more, knowledge of density and pressure yields tbc temperature. In the troposphere, at height where the temperature is larger than 250K, the water vapor term in Eq. (4) becomes significant and it is more efficient to solve for water vapor given some independent knowledge of temperature [Kursinski et al., 1995a].

3-GPS RADIO OCCULTATION FEATURES

Details about vertical and horizontal resolution of the technique, and refractivity, temperature, pressure, water vapor or electron density accuracies as a function of height, arc given elsewhere in the literat are [Hardy et al., 1993, Kursinski et al., 1993; Hajj et al., 1994]. In this section we quickly summarize the results of these studies.

Duc to the nature of tbc measurement, which is a pencil-like beam of the electromagnetic signal probing the atmosphere, tbc technique has a much higher vertical and across-beam resolution than horizontal (i.e. along the beam). The vertical resolution of the technique is essentially set by the physical width of the beam where geometrical optics is applicable. This scale is set by the Fresnel diameter which, in vacuum, is given by

$$D_{vacuum} = 2\sqrt{\frac{\lambda R_{GPS} R_{LEO}}{\left(R_{GPS} + R_{LEO}\right)}}\ , \qquad (7)$$

where λ is the signal's wavelength, R_{GPS} and R_{LEO} are the distances of the tangent point (see Fig. 1) to the GPS and LEO respectively. For a LEO, D_{vacuum} is ~1.5 km. In the presence of a medium, due to bending induced on the signal, the Fresnel diameter is ~0.5 near the surface and approaches 1.5 km above 20 km altitude where bending becomes small. When the signal encounters sharp gradients in refractivity due to either water vapor layers near the surface or sharp electron density changes at the bottom of the ionosphere, the Fresnel diameter shrinks to ~200 meters.

A hori zontal resolution scale is set by the length of the beam inside a layer with a Fresnel diameter thickness. This length is 160-280 km for a Fresnel diameter of 0.5-1.5 km.

In the ionosphere, the vertical scale is still set by the Fresnel diameter; however, tbc horizontal scale can extend several thousands of kilometers due to the large vertical extent and scale height of the ionosphere. These features of the ionosphere allow onc to usc tomographic approaches in order to combine information from neighboring occultations to solve for horizontal and vertical structure [Hajj et al., 1994].

Under ideal conditions. when a LEO tracking GPS has a 360° field of view of the Earth's horizon, about 750 occultations per LEO per day can be obtained. However, side-looking occultations (GPS-LEO link > 45° from velocity or anti-velocity of LEO) sweep across a large horizontal region, and the spherical symmetry assumption described in Sec. 2 becomes inaccurate. Discarding side-looking occultations, onc LEO provides up to 500 occultations per clay.

In the case of GPS-MET, only an aft-looking antenna was mounted on the satellite, which reduces the viewing geometry to 1/2 the Earth's limb (±90° from boresight). In addition, in order to calibrate tbc clocks of the occulting transmitter and receiver, one other GPS transmitter and one ground GPS receiver arc required (see Fig. 2; the technique of calibration is described in more detail in the next section). This requirement, in addition to some memory limitations inside the flight receiver, limits the number of occultations to about 100 per day.

A high inclination LEO provides a set of occultations that covers the globe fairly uniformly. This feature is particularly advantageous when comparing LEO-GPS occultation coverage to that obtained from balloon launched radiosondes. A total of about 800 radiosondes arc launched each 12 hours from sites around the world. The vast majority of these sites are over the northern hemisphere continents, particularly Europe and North America. This creates the need for high resolution temperature/pressure/water vapor profiles in the southern hemisphere and over the oceans. The contribution of radio occultation retrievals to climate anti weather modeling should be particularly important in these regions. (Global data provided by spaceborne nadir sounders average over large- 3-7 km- --vertical distances,)

When compared to infrared spaceborne sounders, the radio occultation technique has the advantage of being an "all-weather" system. Namely, it is insensitive to aerosols, cloud or rain due to the relatively large GPS wavelengths. Unlike other techniques such as radiosonde or microwave sounders, where instruments aced constant calibration, the GPS radio occultation provides a self calibrating system, as will be discussed in more detail below. The long term

stability inherent in radio occultation make this an excellent system to keep an accurate record of climate changes.

4-CALIBRATING THE GPS SIGNALS/ISOLATING ATMOSPHERIC EXCESS DELAY

The main observable used in an occultation geometry is the phase change between the transmitter and the receiver as the occulting signal descends through the atmosphere. This phase change is due to (1) the relative motion of the LEO with respect to the GPS, (2) clock drifts of the GPS and LEO and (3) delay induced by the at mosphere. In order to derive the excess at mospheric Doppler shift, one must remove the contribution of the first two effects.

Accurate knowledge of the GPS orbits conies from an overall solution involving all 24 GPS satellites and a global net work of ground receivers. The LEO orbit is determined by usc of other links tracking the non-occulting GPS satellites.

When the occultation is mostly radial (i.e. GPS-LEO link has no horizontal motion out of the occultation plane), the occultation 1 ink descends through the ionosphere and stratosphere at a rate of about 3 knl/see; thus, crossing a Fresnel diameter (see Sec. 3) in about 0.5 seconds. However, in order to investigate sub-Fresnel structure (by examining the diffraction pattern of the received signal's phase and amplitude) and for other purposes (such as eliminating different signals caused by atmospheric multipath in the lower troposphere) the occulting data is taken at a rate of 50 Hz. In order to calibrate the LEO clock, one more GPS transmitter is tracked by the LEO at the same high rate (link 2 in Fig. 2). in addition, in order to calibrate the GPS clocks, a ground receiver tracks both GPS satellites at 1 Hz (links 3 anti 4 in Fig. 2). One can interpolate the lower rate GPS clock solutions to 50 Hz, due to the greater clock stability (of order 10-12 sec/see, as opposed to 10-9 sec/sec for the LEO clock), and the smoothness of the DoD Selective Availability dithering.

Knowing the position of all four participants (i.e. two GPS satellites, one LEO and one ground receiver), and modeling various physical effects such as light travel time, the three spaceborne clocks can be solved for w .r. t. to the ground clock. The net result of the calibration is the excess phase due to the atmosphere as a function of time (see Fig. 3a).

5-DATA ANALYSIS ANI) TEMPERATURE PROFILES

In this section wc show the various steps of processing for a single retrieval in order to understand the basic characteristics of the atmospheric effects on the signal. We then look at statistical differences between two days' worth of occultations and a numerical weather prediction model.

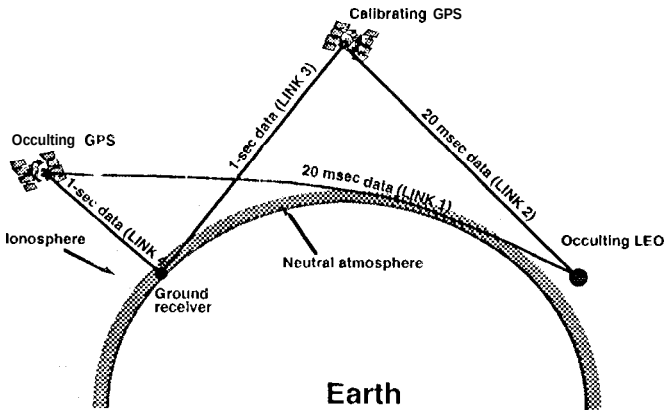

Fig. 2: The. occultation geometry involving two GPS transmitters, one ground receiver and one space receiver.

An Individual Retrieval

After applying the cal i brat ion described in the previous section, we obtain the atmospherically induced phase delay (up to a constant bias). Fig. 3 shows the L1 delay, Doppler shift anti instrumental signai-to-noise ratio for an occultation near Pago Pago, -14 N and 190 E near midnight UT of April 25, 1995. The following features can be observed from these two plots: 1- The phase has a constant bias of about 20 m; this bias is irrelevant for consequent processing si nce it is the phase time derivative that is used. 2- Near the bottom of the ionosphere, there is a sharp fluctuation of the SNK due to the sharp gradient in refi activit y which causes more bending anti therefore defocusing. This is suggestive of the sensitivity of GPS radio occultation to sense the sharp structure of the bottom of the E-layer in the ionosphere. 3- The rapid increase in excess phase anti Doppler shift and the decrease in SNR starting at the lower stratosphere is due to the fact that atmospheric bending is becoming significant. This bending causes the SNR to drop from -130 volt/volt at the top to -35 v/v at the bottom (averaged over 1 sec.), corresponding to about 1i dB of signal loss, anti finally to lose the signal. 4- The SNR shows a clear oscillation near the tropopause which is indicative of a diffraction pattern caused by the sharp change in temperature lapse rate. 5- The SNR shows a peak (-150 v/v) in the middle-troposphere which can be caused by signals coming from a large region (relative to a Fresnel zone) and focusing near the receiver. The corresponding L1 and L2 bending for the same occultation are shown in Fig. 4. Again the sharp feature around 90 km is caused by the sharp curtailing of electron density. The L2 bending as a function of asymptote. miss distance, $\alpha_2(a_2)$, is interpolated to the 1. i asymptote miss distance and the following relation is used to calculate the neutral atmosphere's contribution to bending [procedure suggested by Vorob'ev and Krasil'nikova, 1993]

$$\alpha(a) = 2.54\,\alpha_1(a_1) - 1.54\,\alpha_2(a_1), \qquad (8)$$

where tbc first and second coefficients of Eq.8 corresponds to $f_1^2/(f_1^2-f_2^2)$ and $f_2^2/(f_1^2-f_2^2)$ respectively, and f_1, f_2 are the operating frequencies for L1 and L2 respectively. The difference in bending in L1 and L2 frequencies is due to the dispersive nature of the ionosphere (which leads to Eq. 8). Above 40 km, bending due to the ionosphere dominates.

Using the ionosphere free bending, $\alpha(a)$ and Eqs. (3)-(6), temperature is derived in the neutral atmosphere and is shown as a function of pressure in Fig. 5. Also shown on the same figure are temperature profiles obtained from a nearby radiosonde and a stratospheric numerical weather prediction model obtained from the National Meteorological Center (NMC). The GPS-MET profile agrees with the radiosonde and the NMC analysis to about 2K between 450-1() mbar and to the NMC analysis to about 10 K between 10-1 mbar. The only auxiliary information used in deriving the GPS-MET temperature is an initial condition of temperature at 50 km altitude equal to the NMC analysis temperature. Given the measured density at that height, this initial condition can be translated into a pressure boundary condition which is needed in order to integrate Eq. 6. The oscillation of the GPS-MET temperature above 10 mbar can be attributed to thermal noise in the GPS phase measurement and residual ionospheric effects. The lowest point in the GPS-MET profile corresponds (o about 7 km where the signal is lost. This loss of the signal is due to signal defocusing which is exam-bated by the presence of water vapor layers in the lower troposphere.

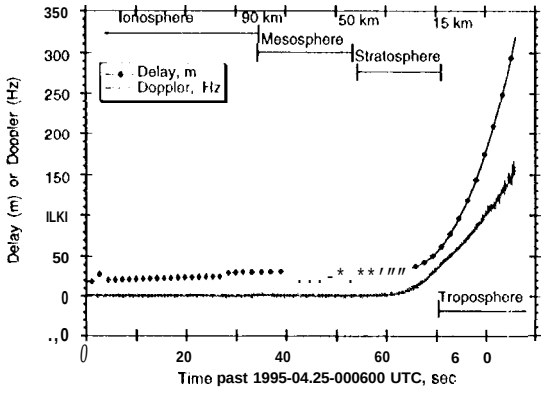

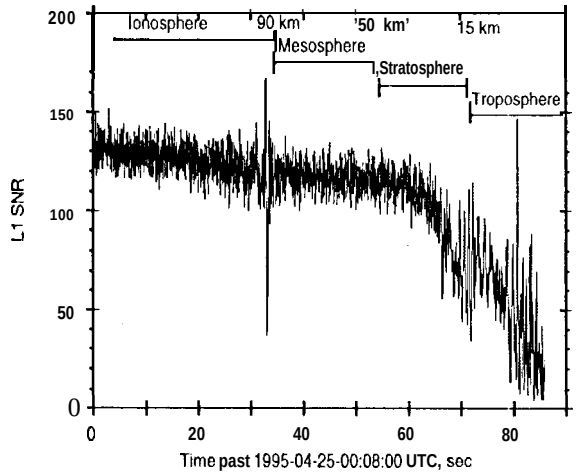

Fig.3: (a) top: excess atmospheric phase and doppler as a function of time; (b) bottom: receiver's signal-to-noise ratio as a function of time

More individual temperature retrievals as well as statistical differences between numerical weather prediction analyses obtained from the European Center for Medium-range Weather Forecasting (ECMWF) and GPS-MET are also discussed by Kursinski et al. [1995 b].

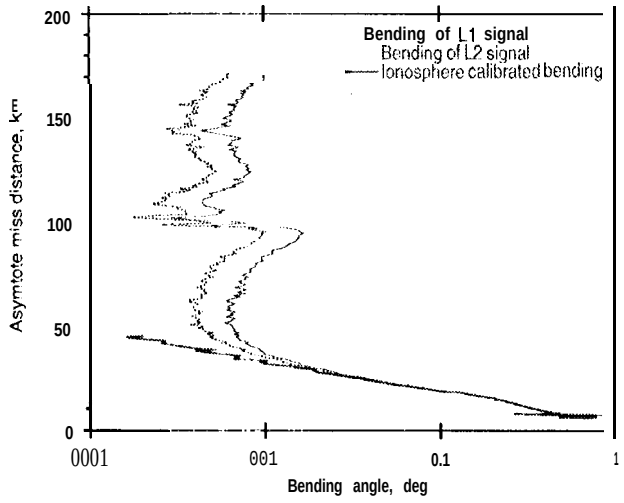

Fig. 4: Bending of GPS-L1 and 1.2 signals and ionospheric free bending as a function of asymptote miss distance

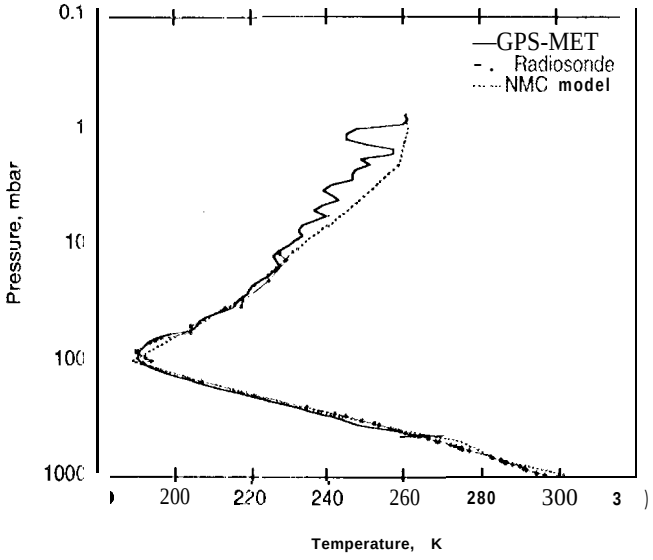

Fig. 5: Temperature profile from GPS-MET radiosonde and NMC stratospheric model

Statistical Comparisons

GPS-MET, which is a secondary instrument on MicroLab 1, is configured in a favorable geometry (antenna boresight in the anti-velocity direction) only for about two weeks out of each repeat cycle of the satellite (55 days). Thus far, this has happened twice: once between April 22-May 6, 1995, and again between June 17-July 11, 1995. (These periods were interrupted by times of non-ideal viewing geometry, clue to attitude control problems.) AS was off during these periods and data for April 24, 25 and May 4, 5 were analyzed. On each of these days respectively, 98, 119, 98 and 69 occultations were recorded, with about half of these successfully inverted, while the rest were automatically discarded, normally due to a data gap in onc of the four links discussed above (SCC Fig. 2). The number of occultations for these four days as a function of the lowest height that an occultation reaches is shown in Fig. 6.

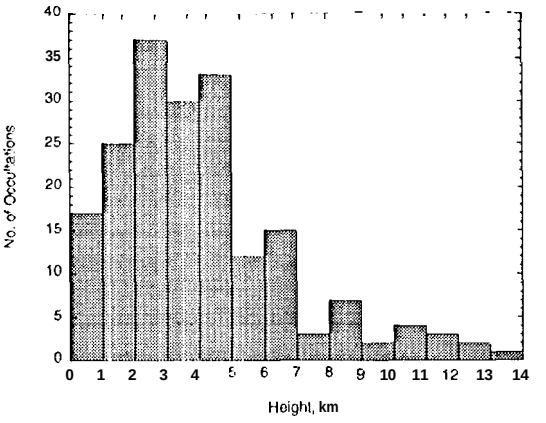

Fig. 6: lowest height of occulting signal for days April 24,25 and May 4,5 of 1995.

In order to assess the accuracies of retrieved temperature profiles from GPS occultations, wc compare with the 6-hour ECMWF analyses. These arc among the best available global analyses of atmospheric temperature structure below 10 mbar, and comparison against them has become a standard method for evaluating the accuracy and resolut ion of observational results [Flobert et al., 199 1]. Fig. 7 shows temperature difference slat istics for all successfully retrieved profiles for May 4 and 5, 1995. in order to eliminate temperature retrieval errors duc to water vapor, t roposphericte mperat arcs exceeding 250 K have been excluded from the comparisons. The three panels in Fig. 7 display temperature difference statistics for the northern high latitudes (30N-90N), the tropics (30S–30N), and the southern high latitudes (30S-90S). Within each latitude zone, retrieved profiles are widely scattered in both location and time.

It is clear from Fig. 7 that agreement between the two data sets in the northern hemisphere is impressive with mean differences of generally less than 0.5 K and difference standard deviations of typically 1 to 2 K. It should also be remembered that these differences include retrieved vertical structure that is not resolved by the ECMWF analysis, especially above 100 mbar. This agreement is particularly significant because the ECMWF analyses are expected to be most accurate in the. northern hemisphere. Although both radiosonde and TOVS (TIROS Operational Vertical

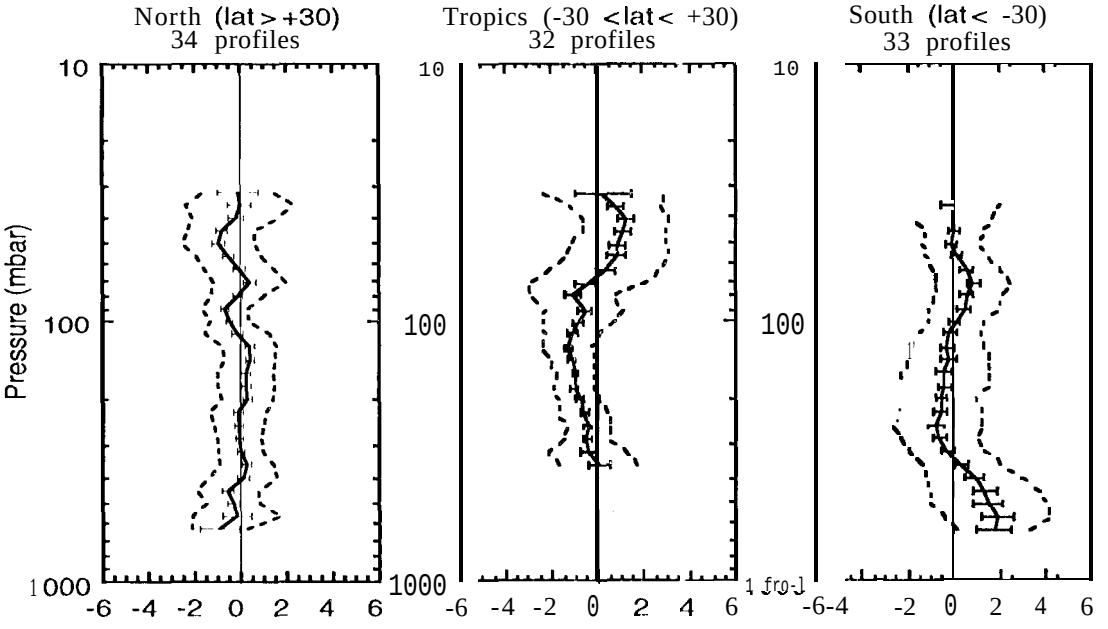

Fig. 7: GPS occultation retrievals from 95/05/04 and 95/05/05 vs. ECMWF analyses. Mean temperature difference with standard error bars (K) (solid lines); One standard deviation about mean difference (shaded lines).

Sounder, a space-based sensors with typical 3-7 km vertical resolution) data are assimilated into the ECMWF model, the analyses are expected to be less accurate in some regions of the southern hemisphere due to the sparse distribution of radiosondes. Southern hemisphere radiosondes cluster over a few land masses whereas the occultations fall mostly over the ocean. Fig. 7 shows that in the southern hemisphere, both mean temperature differences and standard deviat ions increase at lower altitudes. As the occultation retrieval process has little dependence on latitude, the good agreement in the northern hemisphere suggests that the larger systematic and random differences at southern latitudes originate in the analyses rather than in the retrieved profiles. Further inspection of the data shows that this difference feature is produced by a small sub-set of 8 occultation profiles concentrated far from radiosonde ascents in the southern hemisphere storm track and close to the ice edge, where problems in the assimilation of TOVS data arc known to arise [Eyre et al., 1993]. Agreement with the remaining 25 profiles is comparable with that achieved in the northern hemisphere.

Temperature differences at tropical latitudes also display distinctive structure in Fig. 7. On average, retrieved profiles arc about 1 K colder than the analyses between 300 and 100 mbar whereas above 70 mbar, they are warmer by a similar amount. A statistical comparison between tropical radiosondes and the ECMWF analysis revealed a qualitatively similar temperature difference structure, although the radiosonde temperatures in the upper troposphere are generally not quite as cold as the retrievals. Retrieved temperat ure gradients are systematically larger than analysis gradients just above the tropopause. These gradients are associated with wave-like structure often seen in the retrievals just above the tropical tropopause, and not resolved in the ECMWF analyses. While tropospheric standard deviations are similar to those in the northe r n hemisphere, stratospheric values are somewhat larger due, perhaps, to waves above the tropopause. Accurate temperature measurements near the tropical tropopause are needed to understand convection and energy transfer within the atmosphere, troposphere-stratosphere exchange processes, and future climatic variations. Although the temperature retrievals are prelimi nary, and in spite of the clear need for more data, the tropical results are felt to be reliable because of the excellent agreement achieved in the northern hemisphere.

6-IONOSPHERIC PROFILES

Although the purpose of the GPS-MET experiment was mainly to demonstrate the usefulness of the GPS radio occultat ion for sensing the neutral atmosphere, the same technique can be used to obtain profiles of electron density in the ionosphere. 1 n the ionosphere, the spherical symmetry assumption is not as accurate as in the neutral atmosphere, for reasons that are described in Sec. 3. Nevertheless, in this section wc show some representative profile\ of electron densities obtained from GPS-MET with the spherical assumption. A first order, but sign ificant, improvement of the spherical symmetry has been proposed elsewhere [Hajj et al., 1994] where global maps of integrated zenith electron density [Mannucci et al., 1994] can be used in order to constrain the horizontal variability.

The nominal design of the GPS-MET receiver was to collect data at three different rates depending on the geometry of tbc GPS-LEO link. When the link is at posit ive elevat ion (i .e. looking above the LEO local horizontal at 730 km) the rate is 0.1Hz. When the link has a negative elevation (i.e. its tangent point is below the L) :O altitude), data is taken at 1 Hz rate. When the tangent point gets as low as -120 km altitude (30 km

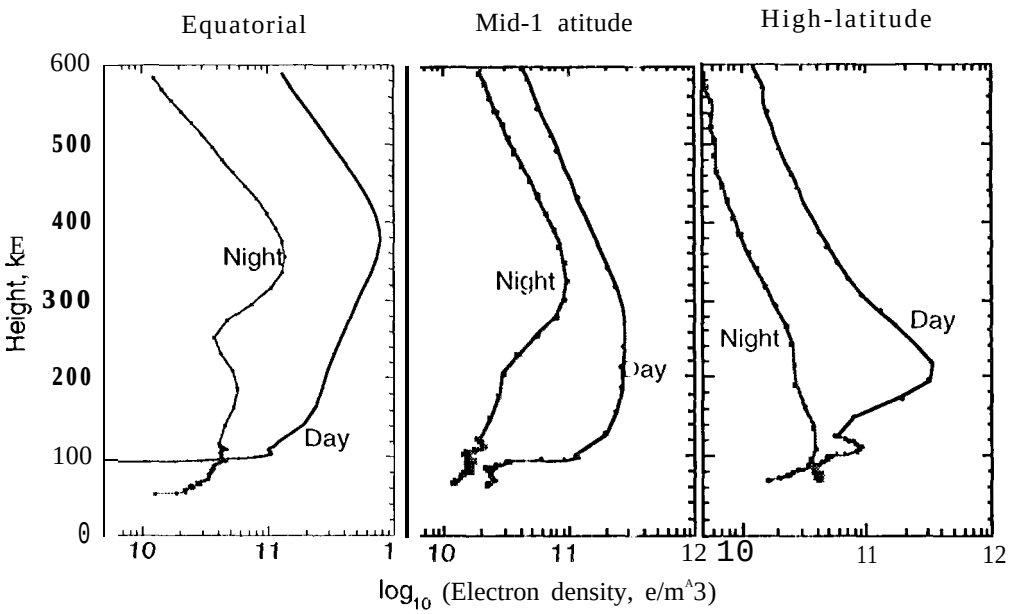

Fig. 9: Ionospheric electron densit y profiles for three different geographical regions for night and day time obtained with the assumption of spherical symmetry.

above which the neutral atmospheric effect starts to be detectable) the data is taken at 50 Hz. (Data used in deriving Fig. 5, had a high rate starting at 180 km.) Due to complications with the receiver software, however, one second data has not been collected. Instead, 0.1 Hz data was available through the ionosphere down to 120 km below which 50 Hz was taken. The inversions shown below are based on connecting these two data rates which explains the higher density of points below 120 km.

One can readily distinguish numerous prominent features of the ionosphere at day and night time and for different geodetic latitudes. These profiles are obtained around midnight (night-time profiles) and noon (day-time profiles) of May 4, 1995. The main features that are readily observed are the presence of the three distinct layers, E, F1 and F2 in the mid-latitude and equatorial day-time profiles, the higher electron density during the day, the sharp drop of the F1 region at night, the higher F2 peak near the equator and the very low peak at high-latitude night. Normally, one would expect the electron density to drop clown to effectively zero around 60 km. The fact that they do not can be attributed to the spherical symmetry assumption used in the retrieval which can create an overall bias in the E-layer electron density, although the point-to-point structure can bc accurate. Ways of improving these retrievals are now underway and will bc presented in a future work.

7-CONCLUSION

Based on theoretical estimations and simulations [Hardy et al., 1993] atmospheric temperature profiles are expected to be accurate to the sub-Kelvin level between 5-30 km heights. initial results of GPS-MET are consistent with these predictions. The GPS radio occultation measurements combine accuracy with the vertical resolution necessary to resolve tropopause structure in a way that is well beyond the capabilities of current space-based atmospheric sounders. A single orbiting GPS receiver provides up to 500 globally distributed soundings daily. The density of these measurements exceeds that of high vertical resolution radiosonde soundings by several factors in the southern hemisphere The coverage, robustness, accuracy, vertical resolution, and insensitivity to cloud inherent to GPS radio occultation suggest that it wiii have a major contribution to global change and weather prediction programs around the globe.

In the ionosphere, GPS radio occultations provide electron density profiles. Spherical symmetry is accurate enough to see the prominent structures in the ionosphere, but improvements over this assumption, such as using information from ground data and/or nearby occultations, can be applied to get more accurate profiles.

ACKNOWLEDGMENTS

We thank M. Exner and R. Ware of UCAR for providing the GPS-MET flight data and Y. Bar-Sever, T. Lockhart, R. Muellerschoen and S. Wu of JPL for their significant contributions. This research was performed at the Jet Propulsion Laboratory, California institute of Technology, under contract with the National Aeronautics and Space Administration.

REFERENCES

Eyer et al., *Quart. J. R. Met. Sm.*, 1 *19:1427-1463*, 1993.

Flobert, J. F. et al., *Mon. Weath. Rev.*, *119:1881-1914*, 1991.

Hajj G. A. et al., *Int. J. of Imaging Sys. and Tech.*, Vol. 5, 174-184, 1994.

Hardy K. R. et al., *Proc. of the ION-GPS* 9.? *Conf.*, Salt Lake City, pp. 1545-1557, 1993.

Kursinski E. R. et al, *Proc. of the 8th Symp. on Meteorological Observations and Instrumentation*, pp. J 153-J158, American Meteorological Society, Anaheim, 1993.

Kursinski E. Ret al, *Geophy. Res. Lett.*, 1995a,

Kursinski E. R. et al, in press, 1995b.

Mann ucci, A. J. et al., *Proc. of the Int. Beacon Satellite Symp.*, L. Kersley cd., University of Wales, Aberystwyth, pp 338-341, July 1994.

Meehan et al, *6th Int. Geodetic Symp. on Satellite Positioning*, Columbus Ohio, 1992.

Melbourne W .G. et al., *GPS geoscience inst rument for EOS and Space Station*, GGI proposal to NASA, July 15, 1988.

Tyler (i. L., *Proc. IEEE*, 75:1404-1431, 1987.

Vorob'ev V.V. and T.G. Krasil'nikova, *Fizica Atmosfery i Okeana, 29, 626-633*, 1993.

Ware R. M. et al, in press, 1995.

Yunck T. P. et al., *Proc. of IEEE position location and navigation symposium*, Orlando, 1988.